

# Evaluation of gas permeation barrier properties using electrical measurements of calcium degradation

Jin Hwan Choi, Young Min Kim, Young Wook Park, Jin Woo Huh, and Byeong Kwon Ju<sup>a)</sup>  
*Display and Nanosystem Laboratory, College of Engineering, Korea University, 5-1, Anam-Dong,  
 Seongbuk-Gu, Seoul 136-713, Korea*

In Sun Kim and Hee Nam Hwang  
*i-Components Co. Ltd., 536-3, Segyo-Dong, Pyongtaek-City, Gyeonggi-Do 450-818, Korea*

(Received 8 March 2007; accepted 14 May 2007; published online 25 June 2007)

In this work, we developed a thin calcium degradation method introducing sensitive electrical resistance monitoring. We have demonstrated structural models of the inorganic/organic thin films to evaluate barrier properties against water and oxygen permeation. The time-dependent transmission curve of a multibarrier coated on both sides of the polyethersulfone substrate had a linear slope which was measured as  $5.17 \times 10^{-3}$  g/m<sup>2</sup> day at 20 °C and 60% relative humidity. This system can measure an accurate permeation rate with a high sensitivity in the measurable range of  $10^1$ – $10^{-6}$  g/m<sup>2</sup> day. In addition, the test structure devised is applicable to various fabrication techniques for passivation layers with durability and ultralow permeability for flexible organic light emitting diodes. © 2007 American Institute of Physics. [DOI: 10.1063/1.2747168]

## I. INTRODUCTION

Organic light emitting diodes (OLEDs) have been widely investigated because of their potential applications in full-color displays, general illuminant light sources, and flexible electronics.<sup>1,2</sup> Flexible electronics, using plastic films, are a growing interest among researchers for use in displays in future embodiments.<sup>1,2</sup> However, the flexible organic devices have a short lifetime property due to water and oxygen permeation through their plastic substrate.<sup>2,3</sup> Many research groups have tried to improve the lifetime and stability of flexible OLEDs (FOLEDs) by using various kinds of passivation techniques that use thin composite polymeric films with single and multistructures.<sup>4–6</sup>

Flexible devices need to be protected from mechanical damage, contamination, and detrimental gases.<sup>7</sup> In organic devices, the organic materials are easily oxidized in the presence of water and oxygen.<sup>5,8–10</sup> The thin cathodes comprising reactive metals are degraded even faster.<sup>8–10</sup> Therefore, developing an extremely impermeable barrier coating technology is a major challenge.<sup>8–10</sup> Bare plastic films such as polyethersulfone (PES) have a too high permeation rate to be used in flexible devices without additional barriers.<sup>6,11</sup> In a single inorganic protection layer, permeation through inorganic film is attributed to defects or pinholes in the film because of the deposition process or the substrate imperfection.<sup>8,12</sup> To prevent such failures, a combination of protective coatings with inorganic and organic materials offers ultralow permeability against gases and, also, applicability for use in flexible and top emissive OLEDs.<sup>5,6,9</sup>

Research reports indicate that a permeation rate of water vapor of below  $10^{-5}$  g/m<sup>2</sup> day is required for

FOLEDs.<sup>2,3,10–13</sup> However, the measurable range of a commonly used system (MOCON Inc., Minneapolis, MN) is limited to  $5 \times 10^{-3}$  g/m<sup>2</sup> day.<sup>1,6,11,14,15</sup> Other test systems have been developed based on mass-spectrometry and radioactivity but these systems are not immediately applicable and at this time have no compatibility.<sup>14</sup> Therefore, the measurements of the ultralow water vapor transmission rate (WVTR) and oxygen transmission rate (OTR) are essential for the development of passivation layers.<sup>12–14</sup>

In this work, we report on a measurement principle including an analysis of an electrical mechanism based on calcium (Ca) degradation. We can measure an accurate gas permeation rate with a high sensitivity and a structural compatibility. In addition, we can demonstrate a fundamental degradation mechanism that can enhance the barrier properties. We have demonstrated the quantitative characterization of the permeation rate for plastic films with single inorganic and multi-inorganic/organic barrier coatings. The structural advantages of the devised test sample enable applications to various kinds of fabrication processes of passivation layers.

## II. EXPERIMENTS

Ca is a reactive material with water and oxygen and also a conductive metal, which has a resistance against an applied voltage.<sup>16</sup> The resistance of the Ca layer is inversely proportional to the amount of average decreasing Ca height if a constant voltage is applied because Ca oxide serves as an insulator. Using these properties, we can derive the permeation rate by using the conductance curve when Ca is oxidized by water permeation through the passivation layer on the plastic substrate. We calculate the WVTR and OTR as

$$\Delta h = \left(1 - \frac{R_i}{R}\right) h_i, \quad (1)$$

<sup>a)</sup> Author to whom correspondence should be addressed; electronic mail: bkju@korea.ac.kr; homepage: <http://diana.korea.ac.kr>

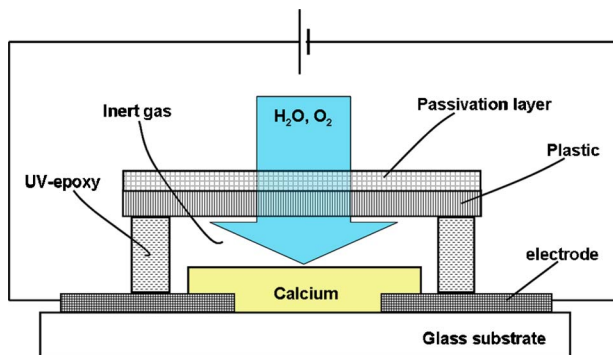


FIG. 1. (Color online) The structure of the Ca permeation test sample.

$$\text{WVTR} = \delta \frac{2M[\text{H}_2\text{O}]}{M[\text{Ca}]} \left(1 - \frac{R_i}{R}\right) h_i \frac{24 \text{ h}}{t}, \quad (2)$$

$$\text{OTR} = \delta \frac{0.5M[\text{O}_2]}{M[\text{Ca}]} \left(1 - \frac{R_i}{R}\right) h_i \frac{24 \text{ h}}{t}, \quad (3)$$

where  $h$  denotes the Ca height,  $R$  is the resistance of the thin Ca layer connected to the electrodes,  $\delta$  is the Ca density, and  $M$  is the molar mass of the indicated reagent.  $R_i$  and  $h_i$  are initial values of  $R$  and  $h$ . The WVTR is proportional to the conductance which is indicated by a decrease in the Ca height  $\Delta h$  versus the elapsed time  $\Delta t$ . Water vapor and oxygen have an independent permeation mechanism. We have established the standard condition (an ordinary atmosphere) of 20 °C and 60% relative humidity (RH).

The test samples were set in Fig. 1. First, a sliver electrode of 250 nm thick and a center Ca layer ( $2 \times 2 \text{ cm}^2$ , 200 nm high) were deposited on a carefully cleaned glass substrate through a shadow mask by a thermal evaporation system below  $10^{-6}$  torr. The ultraviolet (UV) epoxy was dispensed on the edge of the test plastic lid, and the lid was attached to the sample in a glove box system in ambient nitrogen. We used a PES ( $3 \times 3 \text{ cm}^2$  and 200  $\mu\text{m}$  thick) film as an upper plate deposited with passivation layers. The primary factor was that the bare plastic substrate had a higher permeation rate than that of the passivation layer. Also, this substrate could be used with various fabrication techniques for passivation layers.

The thin protective layers were formed onto the PES substrate to evaluate the permeation properties. As shown in Fig. 2, the barrier samples consisted of SiO inorganic material [made by physical vapor deposition (PVD)] and UV-

curable acrylate resin (made by a wet coating process). The transmittance of both inorganic and organic films was higher than 85% (measured by an UV-visible photometer). The test samples were prepared for one side and then both sides, and the single and multipassivation layers on the PES. The barrier coated PES and bare PES samples were made by i-Components (a plastic manufacturing company).<sup>17</sup> Additional UV epoxy was dispensed on the side edge of the film to prevent penetration through the bare plastic side [see Fig. 5(a)]. All of the fabrication processes were performed in a glove box system in ambient nitrogen. Then the test samples were transferred to a climate chamber to control for an environmental condition of 20 °C and 60% RH for a standard measurement. There were two electrodes connected by a two-point probe station to a Keithley 237 multimeter to measure the  $I$ - $V$  characteristics. The measurement voltage was set at 1 mV to minimize the electrochemically enhanced corrosion at a contact interface.

### III. RESULTS AND DISCUSSION

At the beginning of the measurement, water vapor passing through the barrier reacted with the upper Ca atoms, and then CaO was formed. Continual water permeation reacted with the upper end CaO rather than Ca, and then  $\text{Ca}(\text{OH})_2$  was formed. A key fact about this measurement system was that the initial height of the Ca layer was normalized by an initial current when a constant voltage was applied. From these aspects, the resistance corresponded to the average height of Ca.

In fact, the oxidation process was not performed homogeneously. Even the permeation process was generally dominated with defects such as pinholes and microcracks.<sup>8,12</sup> The measurement of the Ca corrosion by using optical properties requires additional work because each passivation layer has a different optical wavelength and the reflection values from each spot are too varied to average. However, using the electrical properties of these phenomena, even the defect distances that were small, like a grain boundary, were detected by a change of the whole resistance. This was because each of the Ca atoms was connected to each other in series; the sum of the volume of each defect had the same resistance as the volume of those defects dispersed homogeneously in connection with the electrical mechanism. So, the slope of current versus elapsed time was linear and represented the average permeation rate. The test structure was designed to

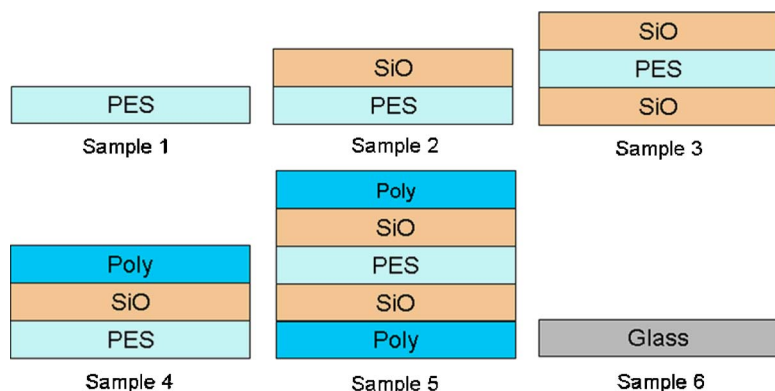


FIG. 2. (Color online) Schematic diagram of barrier coated PES including bare PES and glass.

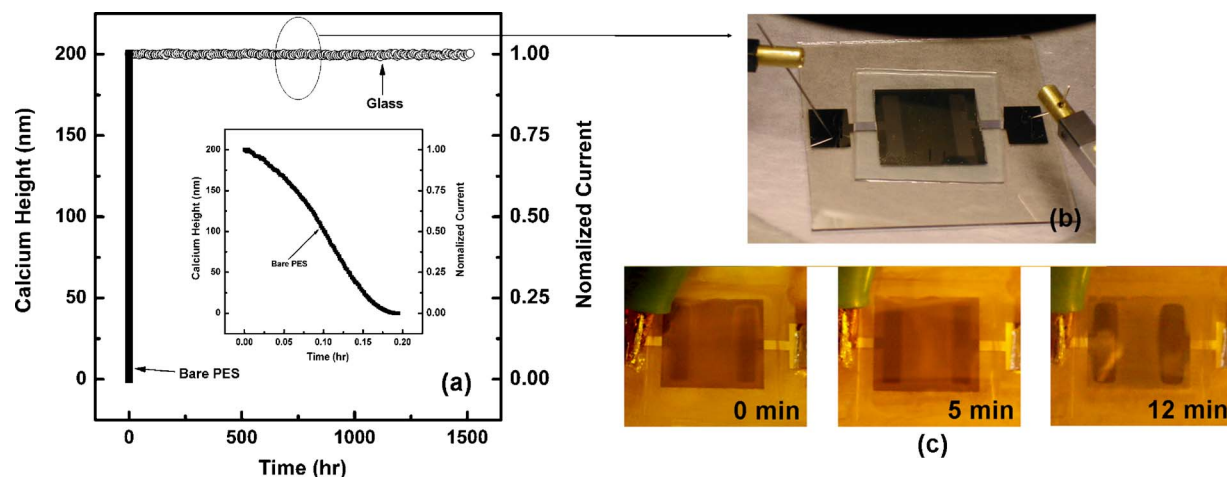


FIG. 3. (Color online) (a) At 20 °C and 60% RH, the permeation curves of bare PES and glass, (b) corresponding measurement image of the glass, and (c) images of Ca corrosion according to water permeation from bare PES.

measure permeation through the passivation layer on a plastic substrate. The permeation through the UV epoxy was desired to be extremely low. The limitation of sensitivity was defined by the permeation through both the UV epoxy and electrodes. The work minimizing the Ca height enabled an increase of the test sensitivity.

The first sample prepared on a glass substrate encapsulated with a glass lid was measured. The permeation rate of a common glass was reported to be below  $10^{-6}$  g/m<sup>2</sup> day. As the substrate of reference, the measurement setup of the glass is depicted in Fig. 3(b). A sensitivity limit was imposed by the quality of encapsulation. The permeation curve of glass encapsulation leads to a stable base-line value of  $<10^{-6}$  g/m<sup>2</sup> day at 20 °C and 60% RH for 1512 h [Fig. 3(a)]. This curve ran parallel to the  $x$  axis. The schematic diagram of the permeation process through the bare PES is shown in Fig. 3(c). The thin Ca (200 nm high) was totally oxidized for 0.2 h at the same condition. The permeation rate of the bare PES film was measured to be 34.1 g/m<sup>2</sup> day, which was a quite higher permeation rate than that of glass.

Therefore, the permeation curve of the bare PES nearly ran in parallel to the  $y$  axis. Therefore, the structural test was performed so that the transmission rate in the range of  $10^1$ – $10^{-6}$  g/m<sup>2</sup> day could be measured to evaluate barrier performance.

As a sensor, the height of Ca could affect the measurement sensitivity. The WVTR equation using a current normalization was verified by comparing Figs. 4(a) and 4(b). Sample 3 was measured at various Ca layers of 100, 200, and 400 nm in height. Figure 4(a) shows the current values against an applied voltage of 1 mV. Each of the current values was normalized to the height of Ca, as shown in Fig. 4(b). As a result, the method using a normalized current value could show that the degradation characteristics of the same samples had parallel slopes and produced consistent permeability, respectively.

The permeation curves for the PES film coated with a single and multibarrier stack are shown in Fig. 2. Samples 2 and 3 were coated with one side and both sides with a SiO single barrier on the PES substrate. In Fig. 5(b), at 20 °C and

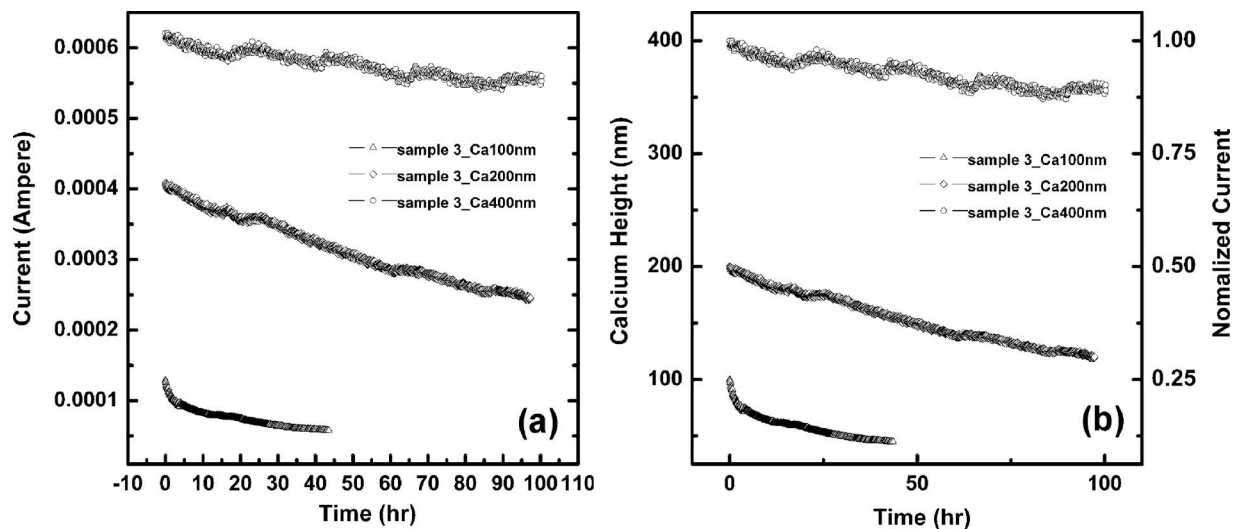


FIG. 4. (a) Degrading current plots of sample 3 according to the change in Ca height. (b) Ca degradation plots derived by the normalized current values show a parallel slope, respectively (at sample 3 at 20 °C and 60% RH).

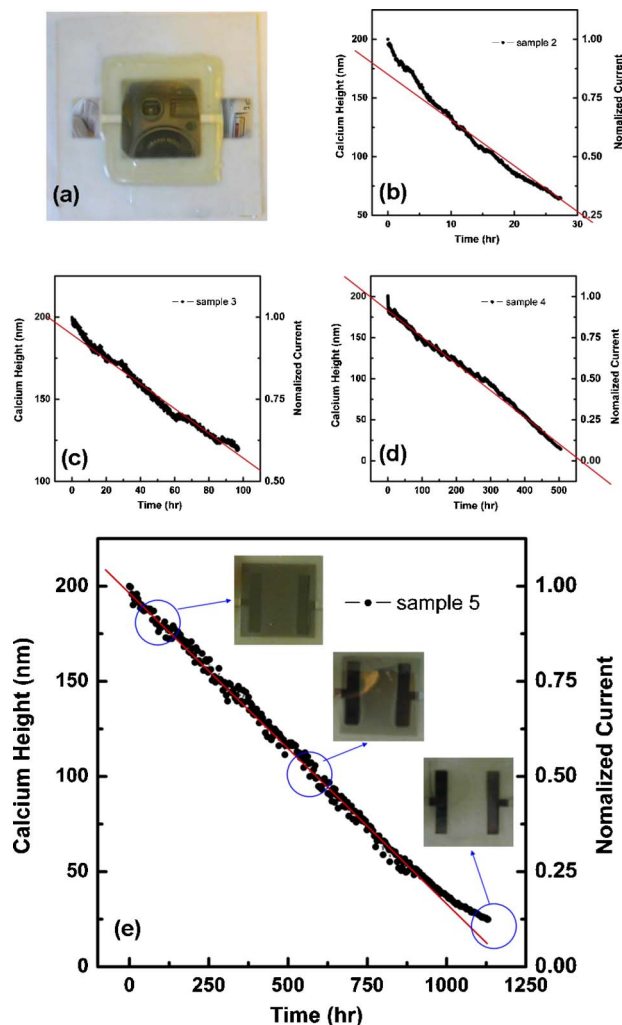


FIG. 5. (Color online) (a) Image of test sample of barrier coated PES and at 20 °C and 60% RH, permeation curves (b) sample 2, (c) sample 3, and (d) sample 4 to evaluate barrier performance. (e) Double-side multilayer coating on PES yields a linear slope, which is  $5.17 \times 10^{-3} \text{ g/m}^2 \text{ day}$ , and optical images of the Ca film according to the permeation plot are shown in the inset image.

60% RH, the permeation plot of sample 2 indicates that the Ca layer of a height of 200 nm was totally oxidized by water vapor for  $\sim 30 \text{ h}$ . We measured a permeation rate with a value of  $1.33 \times 10^{-1} \text{ g/m}^2 \text{ day}$  consistent with the WVTR derivation. The gas transmission through the inorganic materials was commonly considered to be dominated by layer defects such as a microcrack, pinhole defects, and a scratch.<sup>8,12</sup> This result was caused by not just the material performance but also vacuum deposition processes relative to the inorganic material. The permeability of the PES film coated on both sides with a SiO (sample 3) showed an enhanced barrier performance by approximately five times factor in relation to the time dependence function [Fig. 5(c)].

To demonstrate the behavior of a multibarrier inorganic/organic stack, the samples were fabricated to compare their gas barrier properties and degradation mechanism of the test samples. Figures 5(d) and 5(e) show the Ca height-time characteristics according to the normalized current.

These results show that samples 4 and 5 could effectively protect the device from water and oxygen. In addition,

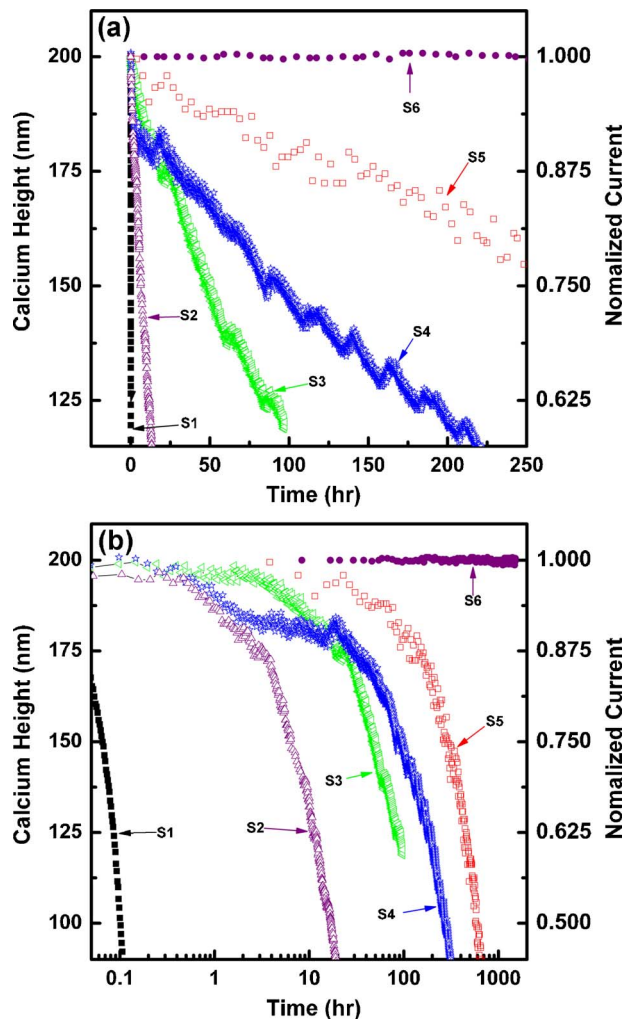


FIG. 6. (Color online) (a) Summarized barrier performances with time-dependent permeation curves and (b) another expression by using a logarithmic scale. “s” means the sample.

the oxidative time of Ca was prolonged as compared to a single inorganic coating technology. Respectively, sample 5 showed a better barrier performance with a permeability value of  $5.17 \times 10^{-3} \text{ g/m}^2 \text{ day}$  at 20 °C and 60% RH, compared to sample 4 with  $1.09 \times 10^{-2} \text{ g/m}^2 \text{ day}$  at the same condition. The images shown in Fig. 5(e) show the change in an optical reflectivity of the Ca film with a permeation process through sample 5.

The above considerations are summarized in Fig. 6(a). Another expression using a log scale to better understand the order functional values of the permeation rate is shown in Fig. 6(b). Table I shows the summarized quantitative results. The structural limit of the test was the permeation of glass encapsulation. The permeation rate of sample 1 (bare PES) through sample 6 (glass) was  $10^1 - 10^{-6} \text{ g/m}^2 \text{ day}$ . Inorganic/organic multilayer stack and double-side coating technology could decrease the permeation rate effectively. One of the advantages in a multi-inorganic/organic passivation technique is flexibility. It is suitable for the FOLEDs and can be effective in prolonging the operational lifetime of the device.

In this work, quantitative WVTRs were measured by using an analysis of the electrical degradation of Ca cells. In this system, a transmission rate in the range of



TABLE I. WVTR at 20 °C and 60% RH determined by the equation. Samples 2–5 show barrier performance data. The glass and bare PES samples are used as references.

Sample No.	WVTR (g/m <sup>2</sup> day) at 20 °C, 60% RH
Sample 1 (bare PES)	$3.41 \times 10^1$
Sample 2 (single one-side coating)	$1.33 \times 10^{-1}$
Sample 3 (single double-side coating)	$2.57 \times 10^{-2}$
Sample 4 (multi-one-side coating)	$1.09 \times 10^{-2}$
Sample 5 (multi-double-side coating)	$5.17 \times 10^{-3}$
Sample 6 (glass)	$<10^{-6}$

$10^1$ – $10^{-6}$  g/m<sup>2</sup> day can be measured. It is particularly useful to evaluate time-dependent barrier properties because the gas permeation rate is determined by the increased resistance versus elapsed time. This method presents a direct comparison of the gas permeability of plastic substrates that are a part of the polymeric passivation layer coating technologies. Inorganic/organic barrier coating and double-side coating technology could decrease water and oxygen permeation rates effectively. Our Ca test sample structure and measurement principle results in a potential application to evaluate the barrier performance for stability of flexible organic electronics.

#### ACKNOWLEDGMENTS

This research was supported by a grant (F0004041-2006-22) from the Information Display R&D Center, one of

the 21st Century Frontier R&D Program funded by Ministry of Commerce, Industry and Energy of the Korean Government.

- <sup>1</sup>M. S. Weaver *et al.*, Appl. Phys. Lett. **81**, 2929 (2002).
- <sup>2</sup>J. S. Lewis and M. S. Weaver, IEEE J. Sel. Top. Quantum Electron. **10**, 45 (2004).
- <sup>3</sup>G. Dennler, C. Lungenschmied, H. Neugebauer, N. S. Sariciftci, M. Lartèche, G. Czeremuszkin, and M. R. Wertheimer, Thin Solid Films **511**, 349 (2006).
- <sup>4</sup>T. W. Kim *et al.*, J. Vac. Sci. Technol. A **23**, 971 (2005).
- <sup>5</sup>Z. Wu, L. Wang, C. Chang, and Y. Qiu, J. Phys. D **38**, 981 (2005).
- <sup>6</sup>S. J. Bae, J. W. Lee, J. S. Park, D. Y. Kim, S. W. Hwang, J.-K. Kim, and B.-K. Ju, Jpn. J. Appl. Phys., Part 1 **45**, 5970 (2006).
- <sup>7</sup>L. Zambov *et al.*, J. Vac. Sci. Technol. A **24**, 1706 (2006).
- <sup>8</sup>S. F. Lim, L. Ke, W. Wang, and S. J. Chua, Appl. Phys. Lett. **78**, 2116 (2001).
- <sup>9</sup>A. B. Chwang *et al.*, Appl. Phys. Lett. **83**, 413 (2003).
- <sup>10</sup>G. L. Graff, R. E. Williford, and P. E. Burrows, J. Appl. Phys. **96**, 1840 (2004).
- <sup>11</sup>S.-H. K. Park, J. Oh, C.-S. Hwang, J.-I. Lee, Y. S. Yang, and H. Y. Chu, Electrochem. Solid-State Lett. **8**, H21 (2005).
- <sup>12</sup>R. S. Kumar, M. Auch, E. Ou, G. Ewald, and C. S. Jin, Thin Solid Films **417**, 120 (2002).
- <sup>13</sup>P. F. Carcia, R. S. McLean, M. H. Reilly, M. D. Groner, and S. M. George, Appl. Phys. Lett. **89**, 031915 (2006).
- <sup>14</sup>R. Dunkel, R. Bujas, A. Klein, and V. Horndt, J. Soc. Inf. Disp. **13**, 569 (2005).
- <sup>15</sup>S. J. Yun, Y.-W. Ko, and J. W. Lim, Appl. Phys. Lett. **85**, 4896 (2004).
- <sup>16</sup>R. Paetzold, A. Winnacker, D. Henseler, V. Cesari, and K. Heuser, Rev. Sci. Instrum. **74**, 5147 (2003).
- <sup>17</sup><http://www.i-components.co.kr/>